



RESEARCH LETTER

10.1002/2017GL072932

Key Points:

- *Sargassum* blooms in the Caribbean Sea lag those in the Central West Atlantic, as determined from MODIS 2000–2016 observations
- A forecast system is established to predict blooms and nonblooms in May–August in the CS by the end of February
- Higher prediction accuracy is found in the eastern CS than in the western CS

Supporting Information:

- Supporting Information S1
- Supporting Information S2
- Text S1
- Movie S1

Correspondence to:

C. Hu,
huc@usf.edu

Citation:

Wang, M., and C. Hu (2017), Predicting *Sargassum* blooms in the Caribbean Sea from MODIS observations, *Geophys. Res. Lett.*, 44, 3265–3273, doi:10.1002/2017GL072932.

Received 8 FEB 2017

Accepted 22 MAR 2017

Accepted article online 24 MAR 2017

Published online 14 APR 2017

Predicting *Sargassum* blooms in the Caribbean Sea from MODIS observationsMengqiu Wang¹  and Chuanmin Hu¹ ¹College of Marine Science, University of South Florida, St. Petersburg, Florida, USA

Abstract Recurrent and significant *Sargassum* beaching events in the Caribbean Sea (CS) have caused serious environmental and economic problems, calling for a long-term prediction capacity of *Sargassum* blooms. Here we present predictions based on a hindcast of 2000–2016 observations from Moderate Resolution Imaging Spectroradiometer (MODIS), which showed *Sargassum* abundance in the CS and the Central West Atlantic (CWA), as well as connectivity between the two regions with time lags. This information was used to derive bloom and nonbloom probability matrices for each 1° square in the CS for the months of May–August, predicted from bloom conditions in a hotspot region in the CWA in February. A suite of standard statistical measures were used to gauge the prediction accuracy, among which the user's accuracy and kappa statistics showed high fidelity of the probability maps in predicting both blooms and nonblooms in the eastern CS with several months of lead time, with overall accuracy often exceeding 80%. The bloom probability maps from this hindcast analysis will provide early warnings to better study *Sargassum* blooms and prepare for beaching events near the study region. This approach may also be extendable to many other regions around the world that face similar challenges and opportunities of macroalgal blooms and beaching events.

Plain Language Summary Blooms of *Sargassum* seaweed appear to have increased in the tropical Atlantic and Caribbean since 2011. These blooms provide important habitats for many marine animals (fish, turtles, shrimps, crabs, etc.) to maintain a healthy marine ecosystem, but large amounts of *Sargassum* deposition on the beaches have caused numerous problems to the local environment, tourism industry, and economy. There is currently little information on *Sargassum* distribution and bloom timing, not to mention a forecast system. In this work, based on satellite measurements and statistics, a forecast system has been developed for the Caribbean Sea. From this system, *Sargassum* blooms in May–August in the Caribbean can be predicted by the end of February, with overall accuracy often exceeding 80% in the eastern Caribbean. The system thus provides at least several months of lead time for the local residents and management agencies to better prepare for potential beaching events. The approach has significant implications for many other regions experiencing macroalgal blooms of either *Sargassum* or *Ulva prolifera*.

1. Introduction

Since 2011, massive *Sargassum* beaching events have occurred in the Caribbean Islands, causing significant environmental and economic problems [Gower *et al.*, 2013; Maurer *et al.*, 2015]. Similar beaching events have also been reported in western Africa and northern Brazil [Oyesiku and Egunyomi, 2014; Széchy *et al.*, 2012]. Although pelagic *Sargassum* provides an important ecological function in the open ocean [Council, 2002; Rooker *et al.*, 2006; Witherington *et al.*, 2012; Lapointe *et al.*, 2014; Doyle and Franks, 2015], large amount of *Sargassum* deposition on beaches can negatively impact the local economy, ecology, and environment [Siuda *et al.*, 2016; Hu *et al.*, 2016]. Usually, massive *Sargassum* deposition on beaches has to be physically removed [Webster and Linton, 2013; Partlow and Martinez, 2015], which represents a management burden as there is often no advanced warning on the amount of *Sargassum* or the timing of beaching events.

These technical obstacles may be overcome through mapping *Sargassum* abundance in the Caribbean Sea (CS) and the Atlantic Ocean and through numerical modeling to predict *Sargassum* growth and transport. While recent advances in satellite remote sensing have made the former possible [Gower *et al.*, 2006; Gower and King, 2011; Gower *et al.*, 2013; Hu, 2009; Wang and Hu, 2016], predicting *Sargassum* blooms in certain locations of the CS requires a thorough understanding of *Sargassum* biology (e.g., growth rate), which may then be coupled with physical forcing (wind- and current-driven transport and dissipation) to model *Sargassum* transport and abundance. Unfortunately, this capacity is currently unavailable due to lack of

sufficient measurement and modeling efforts. Herein, based on remotely sensed *Sargassum* abundance maps, we propose a practical way to predict the likelihood of blooms and nonblooms in the CS. The objective is to provide bloom probability matrices for the CS in May–August based on conditions in the Atlantic in February through hindcast of historical observations; these probability matrices will then provide early warning information by the end of February of every year in the future to assist scientific understanding and management planning (e.g., field surveys, physical removal, and tourism).

2. Data and Methods

2.1. Prediction Concept

The prediction is based on the *Sargassum* distribution maps covering the Central West Atlantic (CWA) and CS derived from Moderate Resolution Imaging Spectroradiometer (MODIS) observations using a recently developed method [Wang and Hu, 2016]. Briefly, MODIS data collected from 2000 to 2016 were processed to Rayleigh-corrected reflectance (Rrc), which was used to derive an Alternative Floating Algae Index (AFAI) for each 1 km pixel [Hu, 2009] that detects the red-edge reflectance of floating vegetation. An automatic feature extraction algorithm was developed to extract *Sargassum* features after masking clouds, cloud shadows, and other artifacts. A linear unmixing scheme was used to determine the subpixel coverage, which was then aggregated to $0.5^\circ \times 0.5^\circ$ grids in each calendar month, resulting in monthly mean *Sargassum* area density (% cover) maps. While Figure 1 shows two sample maps for March 2014 and August 2014, respectively, more maps are presented in an animation in the supporting information, in Figure 2 for bloom years, and in Figure S2 for nonbloom years.

Sargassum blooms appear to develop first in a CWA hotspot region in February–March. Then, following the dominant currents and winds, *Sargassum* in the CWA is transported to the CS in later months where it can develop into a massive bloom. Based on the connectivity and time lag between blooms in the two regions, we hypothesize that blooms and nonblooms in the CS can be predicted from the CWA hotspot region.

2.2. Selection of the Hotspot Region and Bloom Threshold

A hotspot was determined from the multimonth mean using a threshold (Figure S1), where a rectangular region (0° – 8° N, 45° – 29° W) was selected to cover the objectively selected area. For the CS (8° – 23° N, 88° – 59° W), the region was divided into $1^\circ \times 1^\circ$ grids to evaluate the bloom conditions in each grid.

To determine the bloom threshold for each location, mean conditions between 2000 and 2010 (i.e., “non-*Sargassum* years”) were used as the reference. For the CWA hotspot, mean and standard deviation of *Sargassum* density of all February months between 2000 and 2010 were first calculated. Then, for any February in the later years of 2011–2016, if the mean *Sargassum* density was greater than the previously calculated mean plus 2 standard deviations, that February was considered to be a bloom (B) month, otherwise it is a nonbloom (N) month (Figure 1d). Likewise, mean and standard deviation of *Sargassum* density for the CS for each month of May–August were calculated separately from the 2000–2010 MODIS data. Then, for each 1° grid, if *Sargassum* density during a certain month in 2011–2016 was greater than its corresponding mean plus 2 standard deviations, the grid was considered to be a bloom for that month, otherwise a nonbloom (Figure 1c).

2.3. Bloom and Nonbloom Statistics and Prediction Accuracy

First, bloom and nonbloom statistics for the CS and the CWA hotspot region were established. Then, the prediction of bloom or nonbloom in the CS was carried out in a hindcast mode as follows: if there was a bloom (or nonbloom) in the CWA hotspot region in February, it was predicted that there would be a bloom (or nonbloom) in each grid of the CS in each month of May–August of the same year. Finally, the accuracy of the prediction was evaluated using the above bloom and nonbloom statistics with a suite of statistical measures.

Specifically, for each 1° grid in the CS, time series of blooms and nonblooms for each month of May–August between 2007 and 2016 were first generated using the bloom threshold of that month. An example for the month of August is shown in each row of the top left table in Figure 3 part II. Similarly, time series of blooms and nonblooms in the CWA hotspot region in the month of February were also generated using the bloom

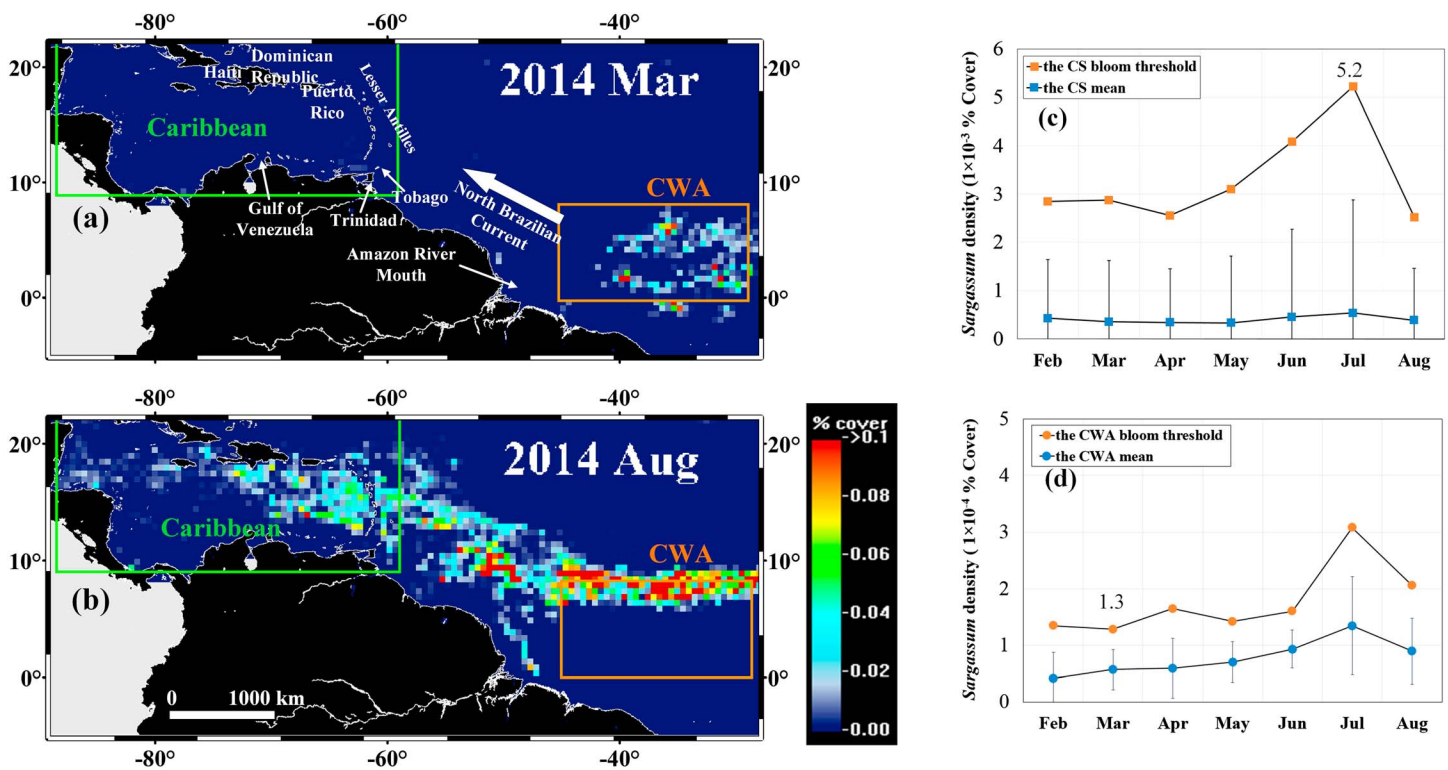


Figure 1. *Sargassum* area density (% cover) maps in (a) March 2014 and (b) August 2014 derived from MODIS observations [Wang and Hu, 2016], suggesting *Sargassum* transport from the CWA to the CS following dominant winds and currents (white arrow). The green box and orange box delineate the CS and CWA hotspot regions, respectively. (c and d) *Sargassum* density thresholds used to determine blooms and nonblooms in the $1^{\circ} \times 1^{\circ}$ grids of the CS and in the CWA hotspot region, respectively. Vertical bars represent standard deviations of each month of 2000–2010 (nonbloom years). The bloom threshold was determined as the mean plus 2 standard deviations. For example, in July, if the density in any grid in the CS is $>5.2 \times 10^{-3}\%$, it is considered as a bloom in that grid; in March, if *Sargassum* density in the CWA hotspot is $>1.3 \times 10^{-4}\%$, it is considered as a bloom.

threshold of February for the CWA hotspot region (top left table in Figure 3 part II). The month of February was selected to be the “predicting” month.

The accuracy of these predictions was evaluated using several statistical measures including the user’s accuracy, producer’s accuracy, overall accuracy, and kappa coefficients [Story and Congalton, 1986; Congalton, 1991]. The equations of the accuracy assessment, as well as examples for four locations in the CS, are listed in the tables of Figure 3. The overall accuracy tells the overall agreement between prediction and ground truth (i.e., observation), and it is defined as the sum of all correct predictions (diagonal elements in the tables) divided by the total number of observations. For a specific grid, X_{NB} (pink color in all tables) is the number of observations when the CWA hotspot shows nonbloom and therefore predicts nonbloom in the CS but the CS grid shows a bloom. X_{NN} (blue), X_{BN} (yellow), and X_{BB} (green) are defined in the same way. The user’s accuracy of bloom prediction is defined as the number of correct bloom prediction (X_{BB}) divided by the total number of bloom prediction ($X_{BN} + X_{BB}$). The user’s accuracy of nonbloom prediction is defined as the number of correct nonbloom prediction (X_{NN}) divided by the total number of nonbloom prediction ($X_{NN} + X_{NB}$). The producer’s accuracy of bloom or nonbloom prediction is defined similarly, but with the total number of observations (in the CS) instead of total number of predictions used in the denominator (Figure 3).

Kappa analysis was also preformed to all 1° grids to calculate the kappa coefficient [Cohen, 1960; Congalton, 1991], which measures the difference between the actual agreement (i.e., the overall accuracy) and the chance agreement (i.e., expected agreement). In this study, kappa coefficient measures the overall difference between the proposed prediction and a random guess. A kappa coefficient of 0 means that there is no difference between prediction and random guess. Larger kappa indicates better prediction performance. Conditional kappa, which can test the individual category agreement [Coleman, 1966; Light, 1971], was also calculated to help interpret the prediction accuracy. Conditional kappa measures the difference between prediction for a certain category (i.e., bloom or nonbloom) and random guess for that category.

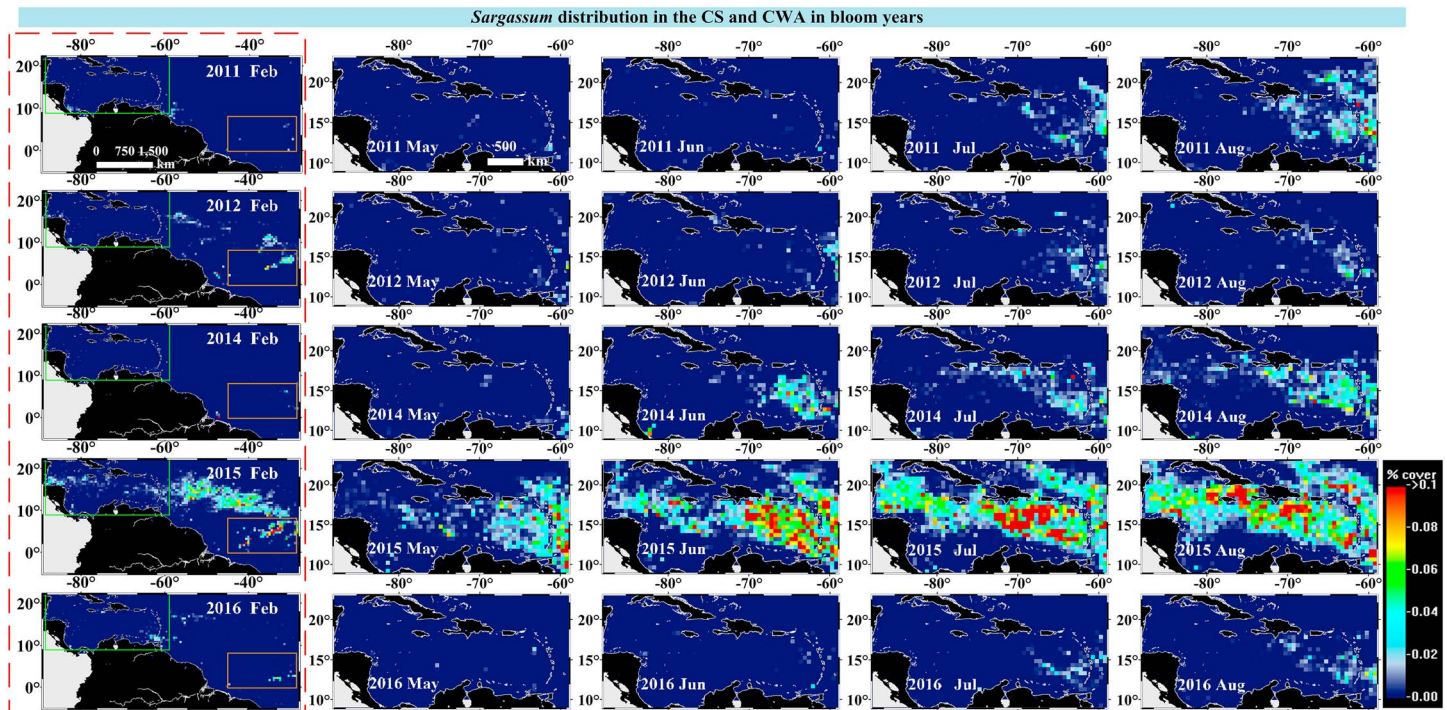


Figure 2. Monthly mean *Sargassum* density maps for bloom years between 2007 and 2016 (2007–2010 and 2013 are nonbloom years). Land and coastlines are masked in black and white, respectively. A value of 0.05 indicates 0.05%. The red dashed box marks the February maps used for the prediction.

3. Results

From 2007 to 2016, 5 years were classified as bloom years (2011–2016 except 2013), and 5 years were classified as nonbloom years (2007–2010, 2013) (Figure S3). Figure 4 shows the summary results of hindcast prediction accuracies for each month of May–August.

Generally, the conditional kappa and user's accuracy show consistent results in terms of overall trend and spatial patterns, but kappa-like measures are less interpretable than user's accuracy. For example, in the top left image of Figure 4 (prediction of bloom in the CS in May), the bottom right corner (near Trinidad) shows a value of 0.60 (orange color). This means that if a May bloom is predicted for this location at the end of February, the odds of a bloom developing there are 60%. Likewise, if a May bloom is not predicted, the odds of a correct prediction are >90% (second image set in Figure 4). Because the interpretation of user's accuracy for both bloom and nonbloom predictions is straightforward, the user's accuracy is recommended for future predictions.

The user's accuracy for nonbloom prediction (mostly >90%) is much higher than for bloom prediction (mostly <50%). This is because most 1° grids in the CS did not have blooms between May and August (Figure 2) regardless of the February conditions in the CWA hotspot. For this reason, for bloom predictions the producer's accuracy and overall accuracy are much higher than the user's accuracy, but for nonbloom predictions the user's accuracy is much higher than the producer's accuracy. These observations may vary between regions and months. For example, for the month of August and near the Lesser Antilles Islands, the user's accuracy of bloom prediction can reach >80%. The producer's accuracy for bloom prediction in this region is also high, suggesting that when a bloom occurs in August near the Lesser Antilles Islands, there is likely a bloom in the CWA hotspot region back in February of the same year. In general, prediction accuracy decreased in the western CS regardless of the accuracy measures, due to a longer distance between the western CS and the bloom source (i.e., the CWA hotspot region).

From these hindcast evaluations, the following findings may be summarized for the prediction of blooms and nonblooms in the CS between May and August using conditions in the CWA hotspot region in February of the same year:

Part I: Accuracy Assessment Equations

		Ground Truth		User's Accuracy
		N	B	
Predicted (CWA)	N	X_{NN}	X_{NB}	X_{N+} X_{NN}/X_{N+}
	B	X_{BN}	X_{BB}	X_{B+} X_{BB}/X_{B+}
Producer's Accuracy		X_{NN}/X_{-N}	X_{BB}/X_{-B}	p_o

$$X_{N+} = X_{NN} + X_{NB}$$

$$X_{+N} = X_{NN} + X_{BN}$$

$$X_{B+} = X_{BN} + X_{BB}$$

$$X_{+B} = X_{NB} + X_{BB}$$

$$N_t = X_{BB} + X_{BN} + X_{NB} + X_{NN}$$

$$\text{Expected Agreement: } pe = \frac{X_{N+} \times X_{+N} + X_{B+} \times X_{+B}}{N_t \times N_t} \times 100\%$$

$$\text{Kappa}_N = \frac{N_t X_{NN} - X_{N+} \times X_{+N}}{N_t X_{N+} - X_{N+} \times X_{+N}}$$

$$\text{Kappa} = \frac{1 - pe}{1 - pe}$$

$$\text{Overall Accuracy: } po = \frac{X_{BB} + X_{NN}}{N_t} \times 100\%$$

$$\text{Kappa}_B = \frac{N_t X_{BB} - X_{B+} \times X_{+B}}{N_t X_{B+} - X_{B+} \times X_{+B}}$$

Part II: Demonstration of the Process to Generate Estimated Accuracy Maps

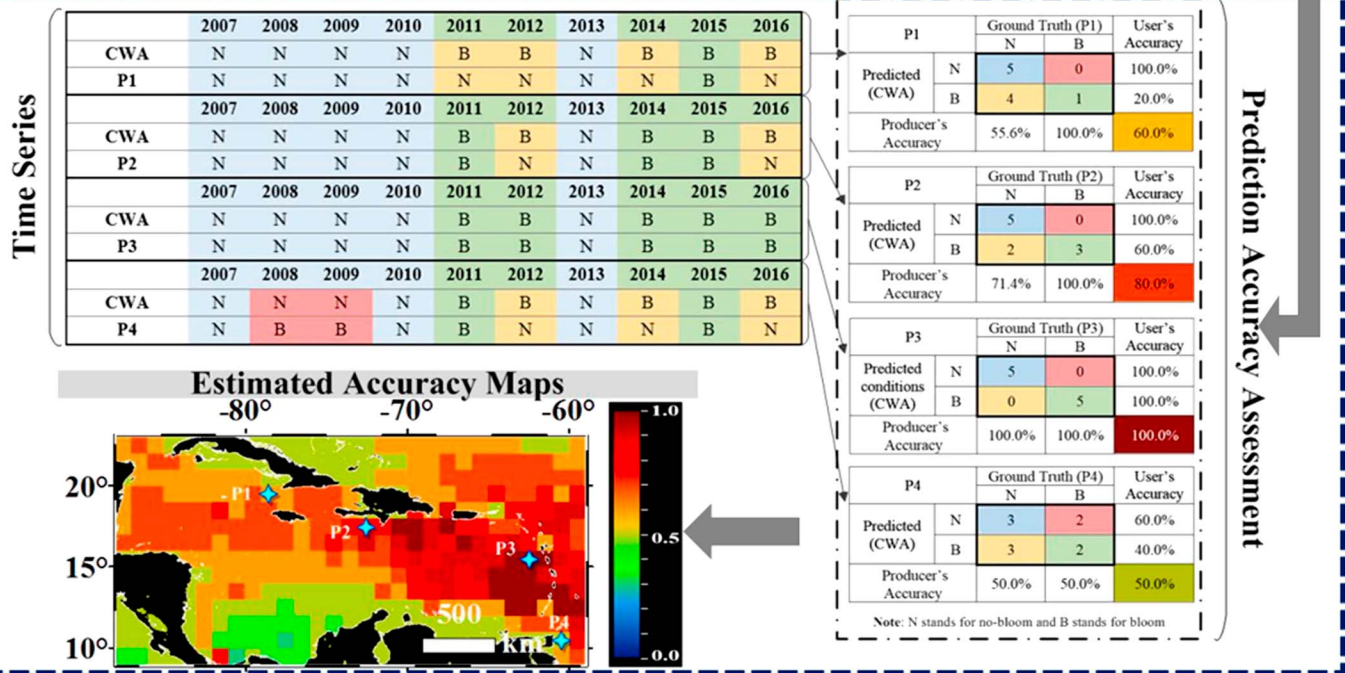


Figure 3. Part I: Illustration of statistical measures to assess prediction accuracy. “B” represents bloom, and “N” represents nonbloom. Part II: Demonstration of the process to generate the estimated accuracy maps. Top left: bloom and nonbloom statistics in the CWA hotspot in February (top rows) and in four locations in the CS in August (bottom rows). Right: accuracy assessment when conditions in February in the CWA hotspot are used to predict conditions in each of the four 1° grids in the CS. The overall prediction accuracy in August for the entire CS is shown in the color coded map, with the four sample locations (P1–P4) annotated.

1. Predicting a nonbloom is much more reliable than predicting a bloom when measured with the user's accuracy.
2. There is a large spatial gradient in the user's accuracy map in bloom predictions, where accuracy in the eastern CS is significantly higher than in the western CS.
3. A similar spatial gradient exists in the overall accuracy map for both bloom and nonbloom predictions, but overall accuracy for the entire CS is much higher than user's accuracy for just bloom prediction.
4. In all predictions, most 1° grids showed kappa coefficient and conditional kappa significantly higher than 0.0, indicating that these predictions have significantly higher success rates than random guesses.

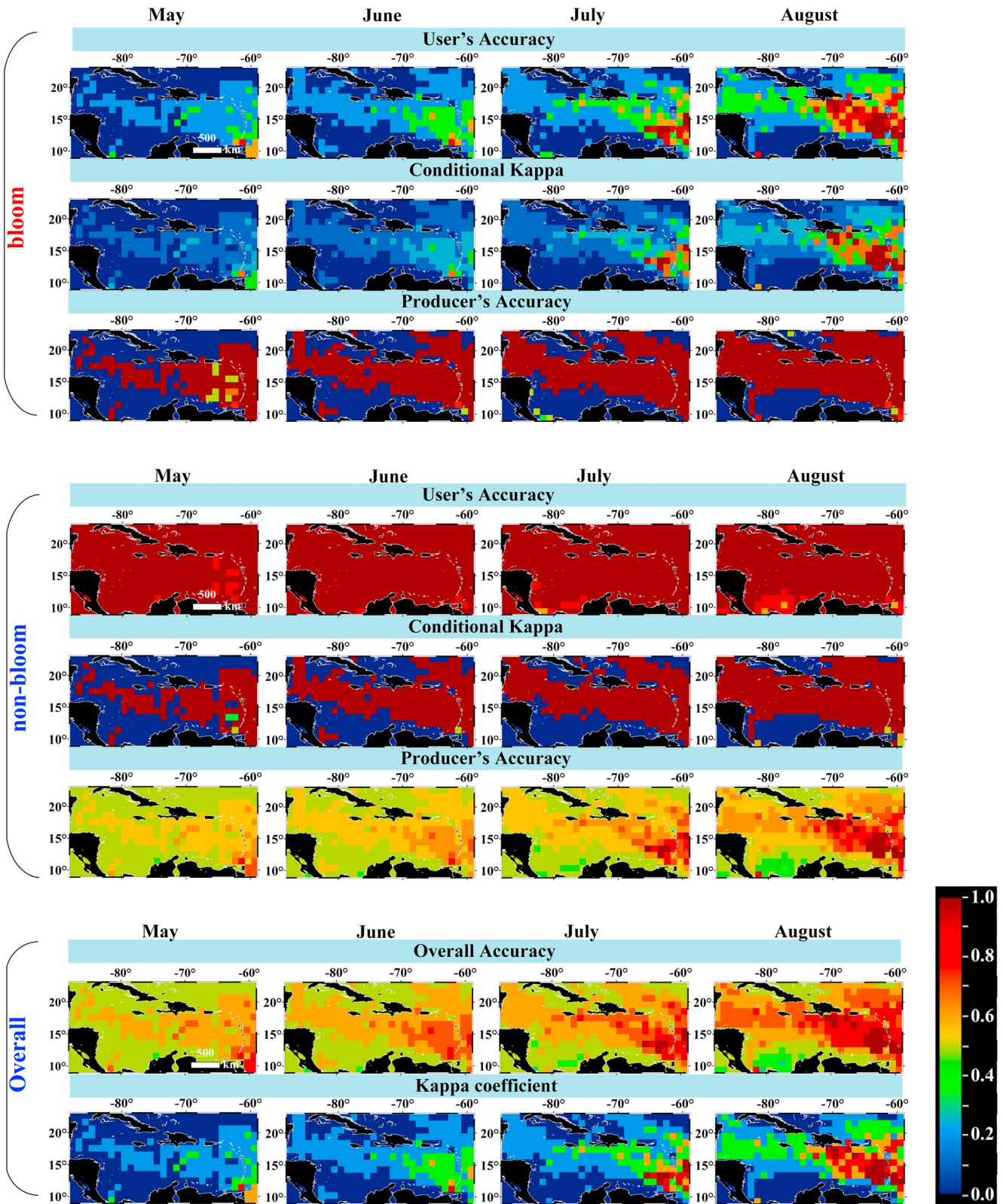


Figure 4. Estimated hindcast prediction accuracy of blooms and nonblooms in the CS between May and August of 2007–2016, based on the bloom conditions in the CWA hotspot region (Figure 1a) in February. Further interpretations of these maps can be found in the text.

5. The accuracy maps shown in Figure 4 may be used as guides for future predictions of bloom and nonbloom conditions in the CS between May and August, where the predictions can be made at the end of February of the same year.

4. Discussion

4.1. Coincidence or Physics Driven

In nature, many phenomena can be highly correlated without a causal effect. The prediction above is based on the fact that if a bloom occurs in one place (CWA), it occurs at a later date in another place (CS), and the same is true for nonbloom. Then, is it simply a coincidence?

The MODIS observations, as shown in the GIF animation in the supporting information, suggest that this correlation is beyond coincidence but driven by physics. Specifically, *Sargassum* in the CS did not initiate locally but from the CWA following the prevailing winds and currents. This observation is supported by the back-tracking results through ocean modeling [Doyle and Franks, 2015; Franks et al., 2011, 2014, 2016; Johnson et al., 2012]. Therefore, the prediction is supported by physics, even though the method is based on statistics.

Because of this, the method provides a simple yet effective way to predict *Sargassum* bloom occurrence in the CS with relatively high accuracy, especially in the windward Lesser Antilles Islands. For a nonbloom prediction, the prediction accuracy is nearly 100% for most locations in the CS. This is because even during bloom years most waters still have low *Sargassum* density. Overall, a nonbloom prediction is more reliable than a bloom prediction in the CS, while the accuracy of a bloom prediction for most windward Lesser Antilles islands can reach >80% in August.

4.2. Prediction Sensitivity

In this work data between 2007 and 2016 were used to estimate prediction accuracy because the numbers of bloom and nonbloom years are balanced during this period. If this period was extended to all MODIS years before 2007, the user's accuracy for bloom prediction would not be affected (Figure S4) because there was no bloom year before 2007. However, because of the extra nonbloom years included, the producer's accuracy for a nonbloom prediction increased significantly, while the user's accuracy for a nonbloom prediction only increased slightly (it is already near 100%). For the same reason, the overall accuracy and kappa coefficient both increased due to the increased number of successful nonbloom predictions. A test was conducted to see whether the month of January–April could be used as the prediction months. Table S1 shows that except for January, all months showed identical bloom conditions in the CWA hotspot, leading to identical prediction accuracy. Therefore, the month of February was determined to be the best prediction month, since it can provide at least 2 months of lead time for local management agencies in the Caribbean.

The work presented here used a binary classification of a bloom or a nonbloom scenario. In reality, blooms will vary in size and intensity. When blooms were further divided into small, medium, and severe blooms according to their intensity, the overall prediction accuracy was lower (Figure S5). However, for a local researcher or manager, knowledge of the bloom/nonbloom probability may be more important than knowledge of the bloom intensity. Therefore, the focus of this study is on the binary classification.

4.3. Applications and Potential Limitations

Although the statistics-based prediction is supported by physics, because the forcing terms (winds, currents, and *Sargassum* growth rate [Webster and Linton, 2013; Carpenter and Cox, 1974; Lapointe, 1996; Lapointe et al., 2014; Ardron et al., 2011; Brooks, 2016; Maréchal et al., 2017]) are not explicitly included in the prediction, the prediction may only be applicable to future years when these forcing terms are similar to the hindcast years used here. The fundamental question is as follows: are the years in this study “normal” years so the prediction can be applied to future normal years?

Time series of the area-averaged surface winds and currents from Windsat and current data from Ocean Surface Current Analyses Real-time (OSCAR), respectively, are plotted in supporting information Figure S6. No significant changes have been observed since 2011 when the first massive *Sargassum* bloom event occurred in the CS. Thus, if future years show winds and currents encompassed by those shown here, the prediction should be applicable.

However, the prediction is *not* on beaching events but on bloom conditions in the CS. It is unknown whether the predictions correlate well with spatial-temporal distributions of beaching events in the CS because this information is not readily available. An online search using the keywords “*Sargassum*,” “Caribbean,” and “Inundation” resulted in 5 news reports in 2011, 2 in 2012, 0 in 2013, 10 in 2014, 28 in 2015, and 2 in 2016, which qualitatively agree with the interannual changes in the observed bloom conditions in the CS. In reality, whether or not a bloom will end up on beaches depends on local winds and currents, which can only be studied through high-resolution modeling or a combination of nearshore daily observations and currents/winds. For example, the *Sargassum* Early Advisory System [Webster and Linton, 2013] used periodic Landsat observations for short-term predictions of potential beaching events, while Maréchal *et al.* [2017] used MODIS daily imagery for the same predictions. Nevertheless, as *Sargassum* blooms are unlikely to diminish in the coming years, the simple forecast system developed here will provide timely information to the Caribbean residents and management agencies on the potentials of *Sargassum* blooms with several months of lead time. Decision makers can benefit from this prediction in several aspects, including improved planning for cleanup, commercial use, and tourism [Hu *et al.*, 2016]. For example, at the time of this writing, a *Sargassum* bloom was found in the CWA hotspot region in February 2017; thus, we predict blooms in the eastern CS in summer 2017. The accuracy of this prediction will be assessed during summer 2017, while the prediction will be sent to interested parties (e.g., NOAA CoastWatch Caribbean and Gulf of Mexico node, Caribbean Coastal Ocean Observing System) through e-mails to provide early alerts.

4.4. Broad Impacts

The study region included the CS and CWA, yet both *Ulva* (a type of green macroalgae) and *Sargassum* macroalgae blooms appear to have increased in recent years all around the world [Smetacek and Zingone, 2013; Qi *et al.*, 2016; Wang and Hu, 2016]. These include those in the Yellow Sea and East China Sea as well as waters off West Africa and north Brazil. Once time series of bloom characteristics and cross-region connectivity are established, the approach developed here could be extended to those regions. The forecasting capacity not only provides early warning to management agencies but also has significant implications for studies of ocean biogeochemistry and ocean ecology as researchers now have at least several months of lead time to prepare for coordinated cruise surveys. Furthermore, *Sargassum* can also be used to extract various products from animal food, biofuel, to plastics, and the U.S. Department of Energy is interested in improved use of *Sargassum* to make these products (<https://vimeo.com/193881420>). One of the potential challenges of such endeavors is to find the *Sargassum* “hotspots” for harvesting at the right time and right location, and the work presented here can help to address this challenge. Indeed, *Sargassum* blooms in recent years have provided both challenges and opportunities to many research and environmental groups [Hu *et al.*, 2016], and a forecasting system represents one significant step toward addressing these challenges.

5. Conclusion

A preliminary forecast system has been developed to predict *Sargassum* blooms in the Caribbean Sea in May–August from bloom conditions in a hotspot region in the Central West Atlantic in February. This is through hindcast analysis of the *Sargassum* distributions derived from MODIS observations between 2000 and 2016 using a recently developed algorithm. Although the prediction is from statistics of bloom and nonbloom occurrence, it is supported by the physical mechanism to drive *Sargassum* transport and by biological factors to drive *Sargassum* growth. Accuracy assessment using historical MODIS observations showed that bloom occurrence in July and August near most of the Lesser Antilles islands can be accurately predicted (up to 80%) at the end of February. Prediction of nonbloom occurrence in most of the CS can be up to 100%. While the data record used to test the prediction is rather short (2000–2016, with only five bloom years in between) and the prediction requires similar environmental forcing factors in future years as in the past years, the forecast system provides a decision support tool to help prepare and make research and management plans with several months of lead time.

References

- Ardron, J., P. Halpin, J. Roberts, J. Cleary, M. Moffitt, and B. Donnelly (2011), Where is the Sargasso Sea? A report submitted to the Sargasso Sea Alliance. Duke University Marine Geospatial Ecology Lab & Marine Conservation Institute. Sargasso Sea Alliance Science Report Series, No. 2, 24.

Acknowledgments

Financial support has been provided by NASA (NNX14AL98G, NNX16AR74G, and NNX17AE57G to Hu) and by William and Elsie Knight Endowed Fellowship (Wang). We thank NASA for providing MODIS data for this analysis. WindSat data were produced by Remote Sensing Systems and sponsored by the NASA Earth Science MEaSUREs DISCOVER Project and the NASA Earth Science Physical Oceanography Program. RSS WindSat data are available at www.remss.com. The OSCAR product was developed by Gary Lagerloef, Fabrice Bonjean, and Kathleen Dohan from Earth and Space Research (ESR). All *Sargassum* relevant imagery data products are available through the *Sargassum* Watch System (SaWS, <http://optics.marine.usf.edu/projects/saws.html>). We thank the two anonymous reviewers for providing detailed and constructive comments to help improve this manuscript.

- Brooks, T. M. (2016), Linking satellite observations with coupled biophysical models of *Sargassum*. *Ocean Sciences Meeting*, New Orleans, La., 22–26 Feb.
- Carpenter, E. J., and J. L. Cox (1974), Production of pelagic *Sargassum* and a blue-green epiphyte in the western Sargasso Sea, *Limnol. Oceanogr.*, *19*(3), 429–436.
- Cohen, J. (1960), A coefficient of agreement for nominal scales, *Educ. Psychol. Meas.*, *20*(10), 37–46.
- Coleman, J. S. (1966), *Measuring Concordance in Attitudes*, pp. 43, Department of Social Relations, Johns Hopkins Univ., Baltimore, Md.
- Congalton, R. G. (1991), A review of assessing the accuracy of classifications of remotely sensed data, *Remote Sens. Environ.*, *37*(1), 35–46.
- Council, S. A. F. M. (2002), Fishery management plan for pelagic *Sargassum* habitat of the South Atlantic region, pp. 228. [Available at <http://safmc.net/Library/pdf/SargFMP.pdf>]
- Doyle, E., and J. Franks (2015), *Sargassum* fact sheet, *Proc. Gulf Caribb. Fish. Inst.*
- Franks, J. S., D. R. Johnson, and D. S. Ko (2016), Pelagic *Sargassum* in the tropical North Atlantic, *Gulf Caribb. Res.*, *27*, SC6-11, doi:10.18785/gcr.2701.08.
- Franks, J., D. R. Johnson, D. S. Ko, G. Sanchez-Rubio, J. R. Hendon, and M. Lay (2011), Unprecedented influx of pelagic *Sargassum* along Caribbean Island coastlines during summer 2011, *Proc. Gulf Caribb. Fish. Inst.*, *64*, 6–8.
- Franks, J., D. Johnson, and D.-S. Ko (2014), Retention and growth of pelagic *Sargassum* in the North Equatorial Recirculation Region (NERR) of the Atlantic Ocean, *Proc. Gulf Caribb. Fish. Inst.*, *67*.
- Gower, J., and S. King (2011), Distribution of floating *Sargassum* in the Gulf of Mexico and the Atlantic Ocean mapped using MERIS, *Int. J. Remote Sens.*, *32*, 1917–1929.
- Gower, J., C. Hu, G. Borstad, and S. King (2006), Ocean color satellites show extensive lines of floating *Sargassum* in the Gulf of Mexico, *IEEE Trans. Geosci. Remote Sens.*, *44*, 3619–3625.
- Gower, J., E. Young, and S. King (2013), Satellite images suggest a new *Sargassum* source region in 2011, *Remote Sens. Lett.*, *4*, 764–773.
- Hu, C. (2009), A novel ocean color index to detect floating algae in the global oceans, *Remote Sens. Environ.*, *113*(10), 2118–2129.
- Hu, C., et al. (2016), *Sargassum* watch warns of incoming seaweed, *Eos Trans. AGU*, *97*, doi:10.1029/2016EO058355.
- Johnson, D. R., D. S. Ko, J. S. Franks, P. Moreno, and G. Sanchez-Rubio (2012), The *Sargassum* invasion of the Eastern Caribbean and dynamics of the equatorial North Atlantic, *Proc. Gulf Caribb. Fish. Inst.*, *65*, 102–103.
- Lapointe, B. E. (1996), A comparison of nutrient-limited productivity in *Sargassum natans* from neritic vs. oceanic waters of the western North Atlantic Ocean, *Oceanogr. Lit. Rev.*, *2*(43), 170.
- Lapointe, B. E., L. E. West, T. T. Sutton, and C. Hu (2014), Ryther revisited: Nutrient excretions by fishes enhance productivity of pelagic *Sargassum* in the western North Atlantic Ocean, *J. Exp. Mar. Biol. Ecol.*, *458*, 46–56.
- Light, R. J. (1971), Measures of response agreement for qualitative data: Some generalizations and alternatives, *Psychol. Bull.*, *76*(5), 365.
- Maréchal, J. P., C. Hellio, and C. Hu (2017), A simple, fast, and reliable method to predict *Sargassum* washing ashore in the Lesser Antilles, *Remote Sens. Appl.: Soc. Environ.*, *5*, 54–63, doi:10.1016/j.rsase.2017.01.001.
- Maurer, A. S., E. De Neef, and S. Stapleton (2015), *Sargassum* accumulation may spell trouble for nesting sea turtles, *Front. Ecol. Environ.*, *13*, 394–395.
- Oyesiku, O. O., and A. Egunyomi (2014), Identification and chemical studies of pelagic masses of *Sargassum natans* (Linnaeus) Gaillon and *S. fluitans* (Borgesen) Borgesen (brown algae), found offshore in Ondo State, Nigeria, *Afr. J. Biotechnol.*, *13*(10), 1188–1193.
- Partlow, J., and G. Martinez (2015), Mexico deploys its navy to face its latest threat: Monster seaweed, *Washington Post*, Oct 28, 2015.
- Qi, L., C. Hu, Q. Xing, and S. Shang (2016), Long-term trend of *Ulva prolifera* blooms in the western Yellow Sea, *Harmful Algae*, *58*, 35–44, doi:10.1016/j.hal.2016.07.004.
- Rooker, J. R., J. P. Turner, and S. A. Holt (2006), Trophic ecology of *Sargassum*-associated fishes in the Gulf of Mexico determined from stable isotopes and fatty acids, *Mar. Ecol. Prog. Ser.*, *313*, 249–259.
- Siuda, A., J. Schell, and D. Goodwin (2016), Unprecedented proliferation of novel pelagic *Sargassum* form has implications for ecosystem function and regional diversity in the Caribbean. *Ocean Sciences Meeting*, New Orleans, La., 22–26 Feb.
- Smetacek, V., and A. Zingone (2013), Green and golden seaweed tides on the rise, *Nature*, *504*(7478), 84–88.
- Story, M., and R. G. Congalton (1986), Accuracy assessment—A user's perspective, *Photogramm. Eng. Remote Sens.*, *52*(3), 397–399.
- Széchy, M. D., P. M. Guedes, M. H. Baeta-Neves, and E. N. Oliveira (2012), Verification of *Sargassum natans* (Linnaeus) Gaillon (Heterokontophyta: Phaeophyceae) from the Sargasso Sea off the coast of Brazil, western Atlantic Ocean, *Checklist*, *8*, 638–641.
- Wang, M., and C. Hu (2016), Mapping and quantifying *Sargassum* distribution and coverage in the Central West Atlantic using MODIS observations, *Remote Sens. Environ.*, *183*, 350–367.
- Webster, R. K., and T. Linton (2013), Development and implementation of *Sargassum* Early Advisory System (SEAS), *Shore Beach*, *81*(3), 1.
- Witherington, B., S. Hirama, and R. Hardy (2012), Young sea turtles of the pelagic *Sargassum*-dominated drift community: Habitat use, population density, and threats, *Mar. Ecol. Prog. Ser.*, *463*, 1–22.